**Annual Symposium of the Hellenic Nuclear Physics Society**

Τόμ. 26 (2018)

HNPS2018

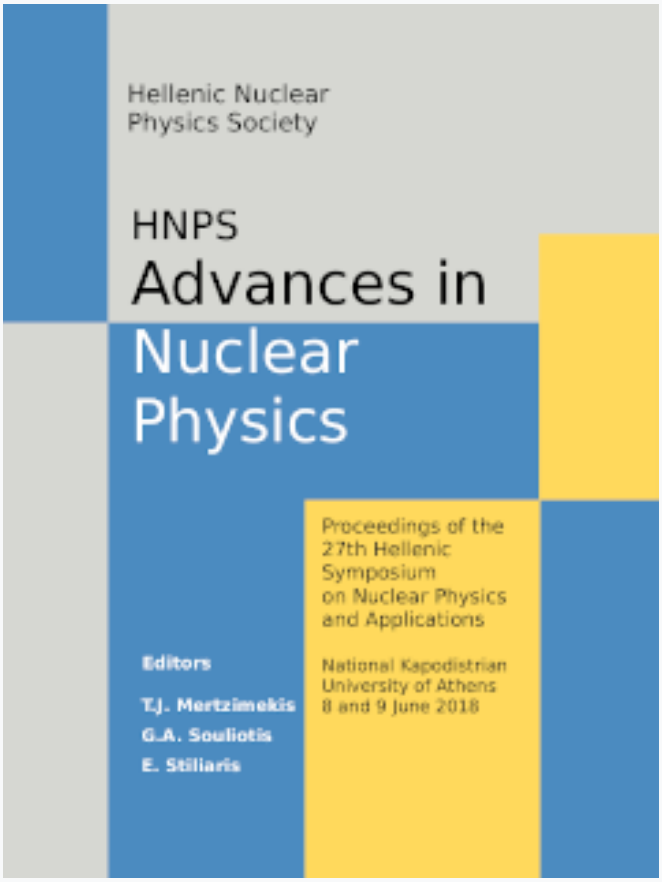


# Constraining new physics from the first observation of coherent elastic neutrino-nucleus scattering

*D. K. Papoulias, T. S. Kosmas*

doi: 10.12681/hnps.1790

# Constraining new physics from the first observation of coherent elastic neutrino-nucleus scattering

D.K. Papoulias[1,*], T.S. Kosmas[2]

[1] *Institute of Nuclear and Particle Physics, NCSR 'Demokritos', Agia Paraskevi, 15310, Greece*
[2] *Theoretical Physics Section, University of Ioannina, GR-45110 Ioannina, Greece*

**Abstract** The process of neutral-current coherent elastic neutrino-nucleus scattering, consistent with the Standard Model (SM) expectation, has been recently measured by the COHERENT experiment at the Spallation Neutron Source. On the basis of the observed signal and our nuclear calculations for the relevant Cs and I isotopes, the extracted constraints on both conventional and exotic neutrino physics are updated. The present study concentrates on various SM extensions involving vector and tensor nonstandard interactions as well as neutrino electromagnetic properties, with an emphasis on the neutrino magnetic moment and the neutrino charge radius. Furthermore, models addressing a light sterile neutrino state are examined, and the corresponding regions excluded by the COHERENT experiment are presented.

**Keywords** Coherent Elastic Neutrino-Nucleus Scattering, Non-Standard Neutrino Interactions, Electromagnetic Neutrino Properties, Sterile Neutrinos

## INTRODUCTION

The observation of coherent elastic neutrino-nucleus scattering (CEvNS) was reported for the first time by the COHERENT experiment at the Spallation Neutron Source (SNS) [1], more than four decades after its initial prediction [2]. A good agreement with the Standard Model (SM) expectation was obtained for neutral currents within a period of 308.1 live days, during which the COHERENT experiment detected neutrinos generated from pion decay, scattered off a low-threshold sodium doped CsI[Na] scintillator , at the $6.7\sigma$ confidence level. Such a breakthrough discovery—apart from completing the SM picture of neutrino interactions with nucleons and nuclei—stands out as a prime motivation to search for new phenomena beyond the SM [3], opening a window towards unraveling some of the most fundamental questions in astroparticle and nuclear physics.

In this work we first perform simulations of the CEvNS spectrum recently recorded by the COHERENT experiment on the basis of our nuclear physics calculations. Then, we explore the sensitivities to various parameters within and beyond the SM by assuming a class of different exotic interactions. Specifically, one of our main aims is to update the previous constraints within the framework of models involving NSIs, neutrino magnetic moments, the neutrino charge radius and sterile neutrinos.

* Corresponding author, email: dimpap@cc.uoi.gr

## BASIC FORMALISM FOR NEUTRINO-NUCLEUS SCATTERING

The SM prediction for the differential cross section of CEvNS with respect to the nuclear recoil energy $T_N$, for neutrinos with energy $E_\nu$ scattered off a nuclear target $(A, Z)$ and ignoring negligible $(T_N = E_\nu)$ terms, can be written in the form [4]

$$\frac{d\sigma_{\mathrm{SM}}}{dT_N}(E_\nu, T_N) = \frac{G_F^2 M}{\pi}\left[(Q_W^V)^2\left(1 - \frac{MT_N}{2E_\nu^2}\right) + \left(Q_W^A\right)^2\left(1 + \frac{MT_N}{2E_\nu^2}\right)\right] F^2(T_N), \quad (1)$$

where GF is the known Fermi coupling constant and M is the nuclear mass. The vector $(Q_W^V)$ and axial-vector $(Q_W^A)$ weak charges read [5]

$$\begin{aligned} Q_W^V &= \left[g_p^V Z + g_n^V N\right], \\ Q_W^A &= \left[g_p^A(Z_+ - Z_-) + g_n^A(N_+ - N_-)\right], \end{aligned} \quad (2)$$

where $Z_-$ $(N_-)$ denote the number of protons (neutrons) with spin up $(+)$ and spin down $(-)$, respectively, while $g_p^A$ $(g_n^A)$ stand for the axial-vector couplings of protons (neutrons) to the $Z^0$ boson. For most nuclei the axial contribution is tiny since the ratio $Q_W^A/Q_W^V \sim 1/A$, while for spin-zero nuclei it holds that $Q_W^A = 0$. In the rest of this work, focusing on the CsI detector, we safely neglect the axial-vector part in Eq.(1), and the differential cross section is enhanced by the coherent superposition of single-nucleon cross sections through the vector SM weak charge $Q_W^V$. The corresponding vector couplings of protons $(g_p^V)$ and neutrons $(g_n^V)$ to the $Z_0$ boson are expressed through the weak mixing angle $\sin^2\theta_W = 0.2312$ by the known relations $g_p^V = 1/2 - \sin^2\theta_W$ and $g_n^V = -1/2$. Thus, within the SM, CEvNS is flavor blind and scales with $\sim N^2$. In Eq. (1), the finite nuclear size suppresses the cross-section magnitude through the Helmtype nuclear form factor [6]

$$F(Q^2) = \frac{3j_1(QR_0)}{QR_0}\exp\left[-\frac{1}{2}(Qs)^2\right], \quad (3)$$

where $j_1(x)$ denotes the first-order spherical-Bessel function and $-q^\mu q_\mu = Q^2 = 2MT_N$ is the momentum transfer during the scattering process. Here, $R_0^2 = R^2 - 5s^2$, with $s = 0.5$ fm and $R = 1.2A^{1/3}$ fm denoting the surface thickness parameter and the effective nuclear radius, respectively.

During the first run of the COHERENT experiment, the total number of protons on target (POT) delivered to the liquid mercury target was $N_{POT} = 1.76 \times 10^{23}$. The SNS neutrinos, produced via the pion decay chain, correspond to an average production rate of $r = 0.08$ neutrinos of each flavor per proton. Specifically, pion decay at rest (DAR-π) $\pi^+ \to \mu^+\nu_\mu$ produces monoenergetic muon neutrinos $\nu_\mu$ (prompt neutrinos with $E_\nu = 29.9$ MeV), followed by a beam of electron neutrinos $\nu_e$ and muon antineutrinos $\nu_{\bar{\mu}}$ (delayed neutrinos) generated by the subsequent muon decay $\mu^+ \to \nu_e e^+ \bar{\nu}_\mu$. In this analysis we treat separately the form factors entering the Cs and I cross sections and consider the experimental neutrino

energy distributions $\lambda_{\nu_\alpha}(E_\nu)$ taken from Fig. S2 of Ref.[1]. The calculated number of events, after taking into account the detection efficiency $a(T_N)$ (see Fig. S9 in Ref. [1]) of COHERENT, reads [4]

$$N_{\nu_\alpha}^{SM} = \sum_{x=Cs,I} K_x \int_{E_\nu^{min}}^{E_\nu^{max}} \lambda_{\nu_\alpha}(E_\nu) dE_\nu \times \int_{T_N^{min}}^{T_N^{max}} a(T_N) \frac{d\sigma_{SM}^x}{dT_N}(E_\nu, T_N) dT_N , \quad (4)$$

where $K_x = t_{\rm run} N_{\rm targ}^x \Phi_\nu$. The exposure time is $t_{\rm run} = 308.1$ days and the neutrino flux is $\Phi_\nu = \frac{r \mathcal{N}_{\rm POT}}{4\pi L^2}$, where $L = 19.3$ m is the distance from the detector to the DAR-π neutrino source, $r = 0.08$ denotes the number of neutrinos per flavor produced for each proton on target, and $\mathcal{N}_{\rm POT} = N_{\rm POT}/t_{\rm run}$. Here, the number of target nuclei for each isotope $x = Cs, I$ is evaluated in terms of Avogadro's number $N_A$, the stoichiometric ratio $\eta$ of the corresponding atom, and the detector mass $m_{det} = 14.57$ kg as [4]

$$N_{\rm targ}^x = \frac{m_{\rm det}\eta_x}{\sum_x A_x \eta_x} N_A, \quad (5)$$

ignoring tiny contributions from the sodium dopant. In our effort to simulate the COHERENT spectrum, we evaluate the expected number of events with respect to the observed number of photoelectrons $n_{PE}$ recorded by the experiment through the relation $n_{PE} = 1.17\, T_N$ (keV). Our theoretical results are depicted in bins of two photoelectrons in Fig. 1 and are compared with the COHERENT data.

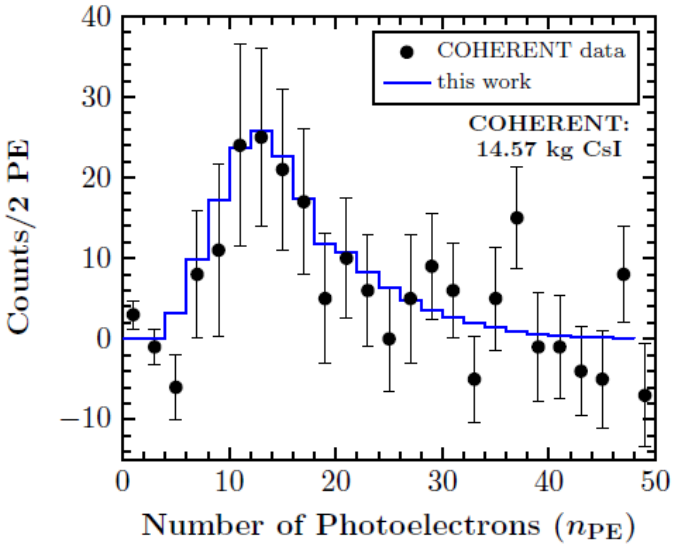


**Fig. 1**. Estimated number of events compared to the COHERENT experimental data

The measurement of CEvNS is widely considered as an important tool for testing

fundamental parameters in the electroweak sector at low energies. At this stage, we are interested in extracting constraints on the weak mixing angle from the recent COHERENT data through a pull test. To this purpose, we perform a sensitivity analysis by varying the value of $\sin^2\theta_W = s_W^2$ and—following the method of Ref. [1]—we treat the measurement as a single-bin counting problem on the basis of the $\chi^2$ function

$$\chi^2(s_W^2) = \min_{\xi,\zeta}\Bigg[\frac{\left(N_{\text{meas}} - N_{\nu_\alpha}^{\text{SM}}(s_W^2)[1+\xi] - B_{0n}[1+\zeta]\right)^2}{\sigma_{\text{stat}}^2} + \left(\frac{\xi}{\sigma_\xi}\right)^2 + \left(\frac{\zeta}{\sigma_\zeta}\right)^2\Bigg], \tag{6}$$

where $N_{\text{meas}} = 142$ is the number of events measured by the COHERENT (see Ref. [1] for details).

Figure 2 illustrates the corresponding limits to the weak mixing angle $\sin^2\theta_W$. This determination of the weak mixing angle is comparable to recent results coming out of global analyses of neutrino-electron scattering data at reactor, accelerator, and Solar neutrino experiments. Despite not being competitive with existing results of parity-violating experiments, such a constraint is extracted for the first time from a low-energy CEvNS measurement.

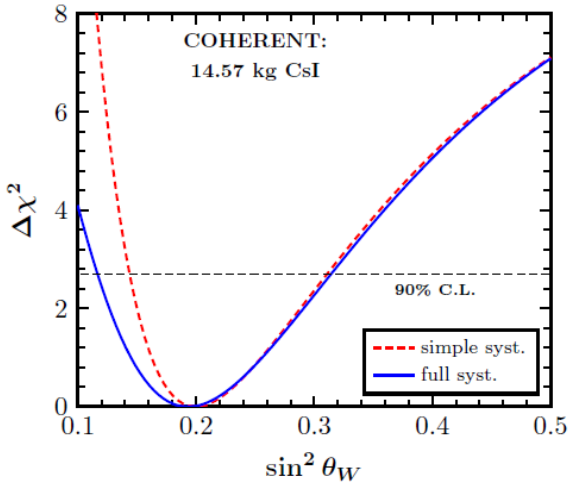


**Fig. 2**. $\Delta\chi^2$ profile of the sensitivity to the weak mixing angle

## CONSTRAINTS ON BEYOND THE SM PARAMETERS

### Nonstandard Interactions

Contrary to the SM case, within the context of nonstandard interactions (NSI) the CEvNS cross section becomes flavor dependent through the substitution $Q_W^V \to Q_{\text{NSI}}^V$ in Eq. (1), where the NSI charge is expressed as [5]

$$Q_{\rm NSI}^{V} = \left(2\epsilon_{\alpha\alpha}^{uV} + \epsilon_{\alpha\alpha}^{dV} + g_p^V\right)Z + \left(\epsilon_{\alpha\alpha}^{uV} + 2\epsilon_{\alpha\alpha}^{dV} + g_n^V\right)N + \sum_{\alpha,\beta}\left[\left(2\epsilon_{\alpha\beta}^{uV} + \epsilon_{\alpha\beta}^{dV}\right)Z + \left(\epsilon_{\alpha\beta}^{uV} + 2\epsilon_{\alpha\beta}^{dV}\right)N\right]. \quad (7)$$

The corresponding new couplings, taken with respect to the strength of $G_F$ , can be either flavor preserving ($\epsilon_{\alpha\alpha}^{qV}$) or flavor changing ($\epsilon_{\alpha\beta}^{qV}$) with $\alpha \neq \beta$. To account for vector NSIs, in Eq. (6) we replace the SM number of events $N_{\nu_\alpha}^{\rm SM}$ with $N_{V,\nu_\alpha}^{\rm NSI}$ and perform a sensitivity analysis in a similar manner to that discussed previously. Focusing on only the nonuniversal terms, through the minimization of the corresponding functions we obtain the sensitivity profiles shown in the left panel of Fig. 3, assuming one nonvanishing coupling at a time. On the other hand, a simultaneous variation of both NSI couplings yields the 90% C.L. allowed regions illustrated in the upper panel of Fig. 4.

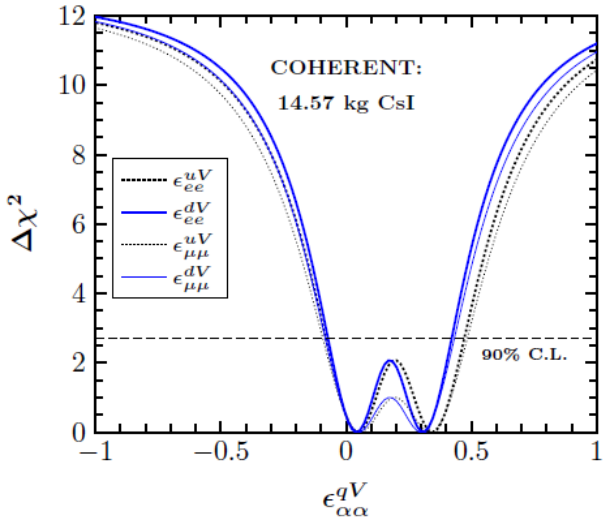


**Fig. 3**. $\Delta\chi^2$ profiles of vector NSI couplings

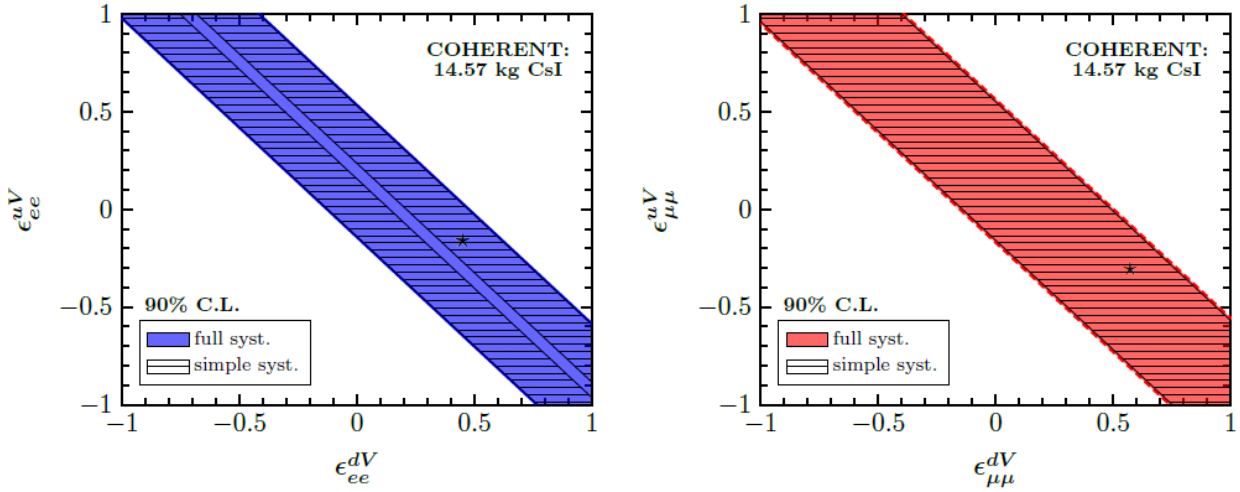


**Fig. 4**. Allowed regions at 90% C.L. of the vector NSI parameters. For comparison, the respective bounds are also presented by assuming a more simplistic sensitivity analysis for the case of vector NSIs. Only the limits corresponding to flavor-preserving nonuniversal couplings are shown, while the best-fit points in each case are denoted by an asterisk

**Electromagnetic Neutrino Properties**

On theoretical grounds, massive neutrinos are well predicted to acquire EM roperties, mainly attributed to the neutrino magnetic moment $\mu_\nu$ and the neutrino charge radius $\langle r_\nu^2 \rangle$. By restricting ourselves to the case of CEvNS, the differential cross section in the presence of a neutrino magnetic moment is given by [4,7]

$$\left(\frac{d\sigma}{dT_N}\right)_{\mathrm{SM+EM}} = \mathcal{G}_{\mathrm{EM}}(E_\nu, T_N)\frac{d\sigma_{\mathrm{SM}}}{dT_N} \tag{7}$$

where the EM contribution—after neglecting axial effects due to the odd-$A$ nuclear species of the COHERENT CsI detector—is obtained through the factor (for details see Ref.[4])

$$\mathcal{G}_{\mathrm{EM}} = 1 + \frac{1}{G_F^2 M}\left(\frac{Q_{\mathrm{EM}}}{Q_W^V}\right)^2 \frac{\frac{1 - T_N/E_\nu}{T_N}}{1 - \frac{MT_N}{2E_\nu^2}}, \qquad Q_{\mathrm{EM}} = \frac{\pi a_{\mathrm{EM}} \mu_{\nu_\alpha}}{m_e} Z. \tag{8}$$

We simulate the expected signal in the presence of EM interactions at the COHERENT detector by analyzing the data through a $\chi^2$ fit and extract the limits to the effective neutrino magnetic moment $\mu_{\nu_\alpha}$. In the left panel of Fig. 5, the relevant $\Delta\chi^2$ profiles are presented by assuming individual measurements of the $\nu_e$ or $(\nu_\mu + \nu_{\bar{\mu},})$ beams, while for comparison the limit for the case of a universal effective neutrino magnetic moment $\mu_\nu$ is also shown. Analogously, a sensitivity test is performed with respect to the neutrino charge radius by fixing the weak mixing angle to the value $\sin^2\theta_W = 0.2312$, as shown in the right panel of Fig. 5. The present constraints are expected to be largely improved with the use of ton- cale detectors.

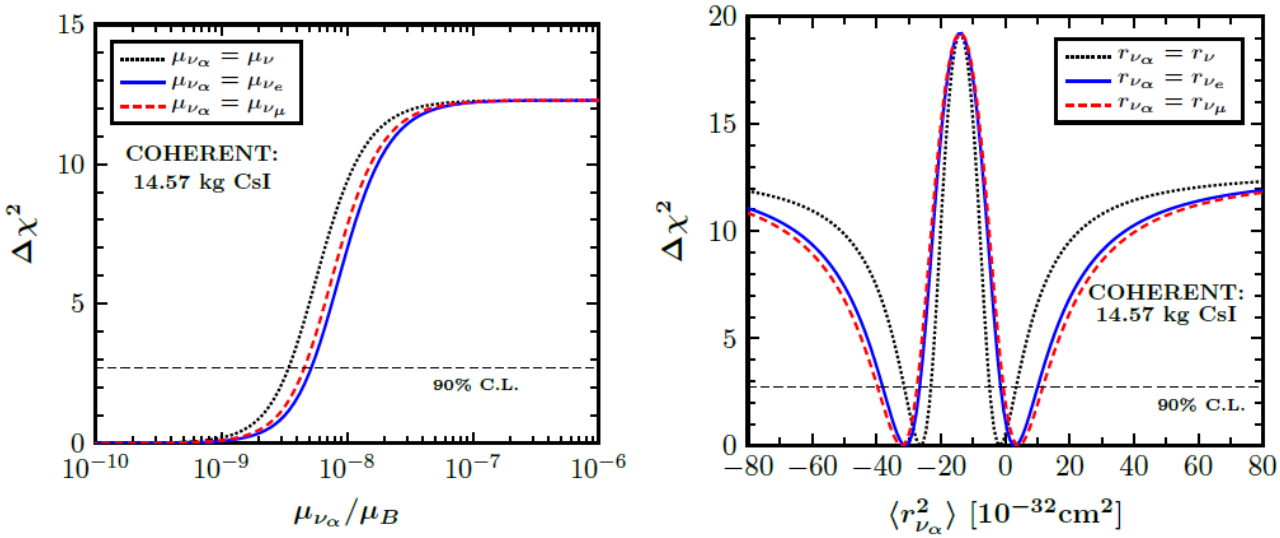


**Fig. 5**. $\Delta\chi^2$profile of the sensitivity to the neutrino magnetic moment $\mu_\nu$ (left panel) and to the neutrino charge radius $\langle r_\nu^2 \rangle$. (right panel) from the analysis of the COHERENT data

**Sterile Neutrinos**

Despite the solid evidence on the number of neutrino flavors implied by the three-neutrino oscillation paradigm [8], existing anomalies (such as those coming from LSND and MiniBooNE data) as well as the controversial predictions for reactor neutrino fluxes have motivated a plethora of phenomenological considerations suggesting potential additional neutrino generations [9,10]. In such theories, the neutrino flavor eigenstates $\nu_\alpha, \alpha = \{e, \mu, \tau, s\}$ and the corresponding mass eigenstates $\nu_i, i = \{1,2,3,4\}$ are related through the usual unitary transformation $\nu_\alpha = \sum_i U_{\alpha i}\nu_i$. In this work we restrict our analysis by considering the simplest (3+1) mixing scheme, which extends the SM with one additional noninteracting sterile neutrino state with a mass of the order of 1 $\mathrm{eV}^2$. For short-baseline (SBL) neutrino experiments, such as COHERENT, the effective survival probability for neutrinos or antineutrinos reads [11]

$$P^{\mathrm{SBL}}_{\nu_\alpha \to \nu_\alpha}(E_\nu) = 1 - \sin^2 2\theta_{\alpha\alpha} \sin^2\left(\frac{\Delta m^2_{41} L}{4E_\nu}\right), \tag{9}$$

with mixing angle $\sin^2 2\theta_{\alpha\alpha} = 4|\mathrm{U}_{\alpha 4}|^2(1 - |\mathrm{U}_{\alpha 4}|^2)$ and mass splitting $\Delta \mathrm{m}^2_{41} = \mathrm{m}^2_4 - \mathrm{m}^2_1$. The extracted bounds with regards to the sterile neutrino oscillation mixing parameters $(\sin^2 2\theta_{\mathrm{new}}, \Delta m^2_{41})$ are demonstrated at 90% C.L. in Fig. 6. Even though within the simplified (3+1) scenario the status of the current limits is poorly constrained, the resulting exclusion curves indicate that CEvNS measurements constitute an excellent probe for studying neutrino mixing beyond the three-neutrino oscillation picture.

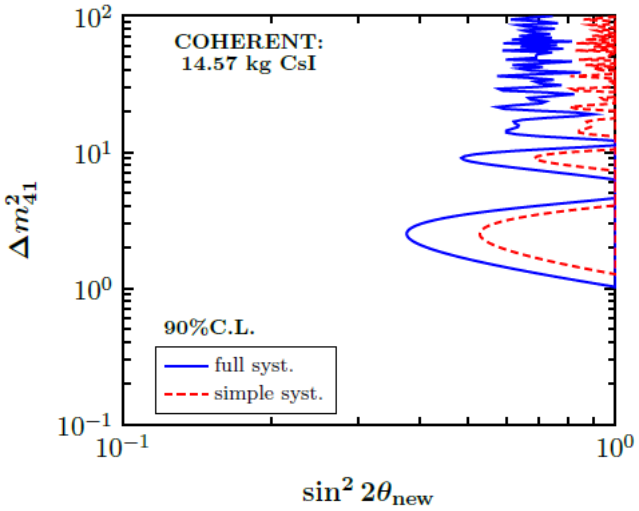


**Fig. 6**. Exclusion curves at 90% C.L. from the analysis of the COHERENT data assuming sterile neutrinos in the 3+1 scheme.

## CONCLUSIONS

We have simulated the COHERENT spectrum and explored several aspects of CEvNS within and beyond the SM, through nuclear physics calculations for the relevant Cs and I isotopes. Special attention has been paid to various contributions to neutrino-nucleus scattering arising within the context of potential NSI, EM neutrino interactions, sterile neutrino mixing models, and the presence of new mediators. In this work, through a

dedicated sensitivity analysis of the recent COHERENT results, the weak mixing angle was determined for the first time from a low-energy CEvNS measurement, constituting an independent SM precision test. Focusing on the aforementioned beyond-the-SM processes, we quantified the corresponding new couplings and presented the regions allowed/excluded by the COHERENT data in the framework of a two-d.o.f. analysis. The latter are complementary to existing limits extracted from neutrino-electron scattering data, while a large improvement is expected from the next phase of the COHERENT experiment on the basis of a multitarget strategy and more massive detectors. Future CEvNS measurements achieved through the deployment of different detector subsystems at the COHERENT suite would be highly efficient at probing the quark content of nucleons, as well as the neutron density distribution in the field of nuclei.

We estimate that in the short term stronger constraints—by up to 2 orders of magnitude—could be placed from a combined analysis of DAR-$\pi$ and ongoing reactor-based CEvNS experiments, with the promising prospect of breaking present degeneracies in NSI models which are very relevant in oscillation and supernova physics, B-meson decay, and Dark Matter studies. The state-of-the-art ultra low-energy detector technologies employed in the relevant projects have the capability to probe EM neutrino properties which may lead to new insights in theoretical models of neutrino mass, while the upcoming CEvNS measurements may offer remarkable probes of sterile neutrinos, competing with existing SBL neutrino oscillation searches.

## References


[1] D. Akimov et al. (COHERENT), Science 357, p.1123 (2017)
[2] D. Z. Freedman, Phys. Rev. D9, p.1389 (1974)
[3] K. Scholberg, Phys. Rev. D73, p.033005 (2006)
[4] D.K. Papoulias, T.S. Kosmas, Phys.Rev. D97, p.033003 (2018)
[5] J. Barranco, O.G. Miranda, T.I. Rashba, JHEP 0512, p.021 (2005)
[6] J. Engel, Phys. Lett. B264, p.114 (1991)
[7] P. Vogel and J. Engel, Phys. Rev. D39, p.3378 (1989)
[8] P.F. de Salas et al., Phys.Lett. B782 p.633 (2018)
[9] A. Anderson, et al., Phys.Rev. D86, p.013004 (2012)
[10] B. Dutta et al., Phys. Rev. D94, p.093002 (2016)
[11] Y. Ko et al., Phys. Rev. Lett. 118, p.121802 (2017)